Pestic. Sci. 1996, **47**, 309–318

A New Binding Model for Structurally Diverse ALS Inhibitors

Toshio Akagi

Central Research Institute, Ishihara Sangyo Kaisha Ltd, 2-3-1 Nishi-shibukawa, Kusatsu, Shiga 525, Japan

(Received 2 October 1995; revised version received 20 December 1995; accepted 8 March 1996)

Abstract: Acetolactate synthase (ALS) has been a very attractive target for herbicides for the last decade. There are several ALS inhibitors in commercial use spanning the world-wide market. In this study, the common structural features within a subset of ALS inhibitors were investigated by molecular graphics and quantum chemical calculations. Satisfactory results were obtained with model calculations based on the presumption that the relative location of the inhibitor azine moiety and some receptor cationic group remained fixed. The cationic group was assumed to interact with an acidic group in each of the inhibitors. This model explains many aspects of ALS inhibitors (sulfonylureas, triazolopyrimidines, pyrimidyl ethers and other classes) such as: (1) the common structural feature among the different classes of ALS inhibitors, (2) the substituent effects in the hydrophobic moiety of each class and (3) the structure–activity relationships of the acidic moiety of each class. These are significant achievements for a model based on in-vivo herbicidal activity and gas-phase calculations, but the model also has its limitations: (1) Only compounds with acidic groups and azine moieties can be addressed, (2) the structure–activity relationships of the hydrophobic moiety are not yet fully understood and (3) only a qualitative prediction of activity levels is possible.

A preliminary trial of ligand design predicted the novel skeleton of an ALS inhibitor that was published independently from this study.

Key words: acetolactate synthase inhibitors, receptor mapping, molecular modelling, pharmacophore, structure–activity relationships, ligand design

1 INTRODUCTION

Acetolactate synthase (ALS; also known as acetohydroxyacid synthase, AHAS) has been a very fruitful target for herbicides over the last decade.[1] Sulfonylureas[2–6] (SUs, Fig. 1) which inhibit this enzyme are very effective for weed control at low rates (10–100 g ha^{-1}). Other series of ALS inhibitors such as imidazolinones[7,8] (IMs, Fig. 2), triazolopyrimidines[9] (TPs, Fig. 3) and pyrimidyl ethers[10] (PEs, Fig. 4) also act at low concentrations. These ALS inhibitors cover the main commercial herbicide markets, including corn, cereals, soybean, rice, cotton and turf. There are some published studies on structure–activity relationships (SAR) of ALS inhibitors.[3,4,6,8] However, since all of them are concerned with only one series of compounds, the common features of ALS inhibitors are not yet clear. Although it is interesting that such structurally diverse compounds bind specifically to the same target protein, no crystallographic data are available for the enzyme–inhibitor complex of ALS. Therefore, in this study, the common three-dimensional structural features[11,12] were investigated using molecular graphics and quantum chemical calculation. Since almost all SUs, TPs and PEs are 4,6-substituted azines (pyrimidines and *s*-triazines) with an acidic substituent at the 2-position, this study focused on the spatial distribution of acidic moieties relative to the azine moieties. In this paper, a binding model for ALS inhibitors is proposed and explanations of some SAR in these series of compounds are given. A preliminary ligand design exercise is also described. To our knowledge, this is the first study to propose a binding model that accounts for the many types of ALS inhibitor, although it does not provide a quantitative understanding of the activity.

Pestic. Sci. 0031-613X/96/$09.00

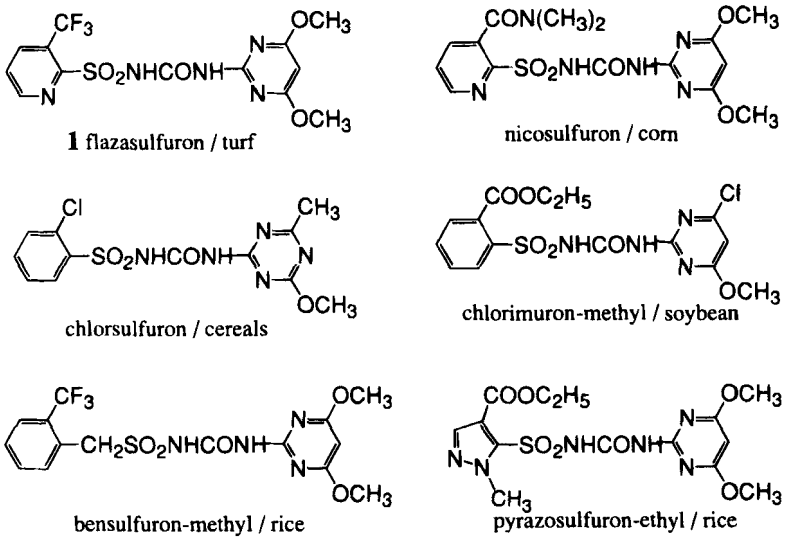

Fig. 1. Chemical structures of sulfonylurea herbicides.

2 DERIVATION OF MODEL

2.1 Atom-by-atom fitting

Three compounds, **1**, **2** and **3** (Figs 1, 3 and 4), were selected, one from each class of ALS inhibitor, in order to examine overlays of the azine moiety and the acidic groups by conventional atom-by-atom fitting. Three-dimensional structures were prepared by semi-empirical quantum chemical calculations with the AM1 Hamiltonian.[13] Atom-by-atom fitting was implemented by the FMFIT algorithm[14] followed by the MAXMIN algorithm[15] utilising the Tripos 5.2 force field.[16] In the MAXMIN algorithm, molecules are superimposed by an energy-weighted fitting procedure that seeks a compromise between low conformational energies and the best overlay. All of the overlays obtained were unsatisfactory. In the best result, the position of the acid group oxygens seriously deviated from each other (rms distance = 1·75 A) when the azine moiety was superimposed.

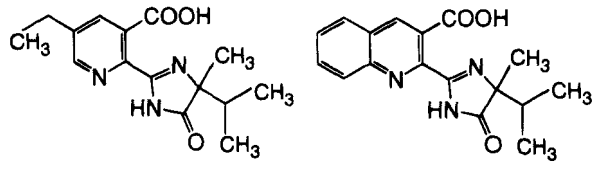

Fig. 2. Chemical structures of imidazolinone herbicides.

2.2 NH_4^+ binding model

The unsatisfactory results from atom-by-atom fitting prompted a change of strategy for the pharmacophore search. The new strategy was to seek a common three-dimensional structure for the presumed receptor functions. Since most ALS inhibitors contain an acidic moiety, it was hypothesised that this binds to a cationic group in the receptor. An NH_4^+ ion was chosen to represent this cationic group for convenience of calculation. The first task in building the model was to determine the position of the NH_4^+ ion relative to the azine (see Fig. 5). The initial position of the NH_4^+ ion was obtained by replacing the acidic proton in the geometry of **3** from the atom-by-atom fitting. Then the total energy calculated by AM1 of the complex of NH_4^+ and **3** was minimised, while the torsion angles $\theta 1$ and $\theta 2$ in Fig. 6 were kept unchanged. The relative geometry of the azine moiety and the NH_4^+ obtained for **3** was used to prepare initial conformations of binding models for **1** and **2**, and it was kept unchanged during energy minimisation of these models.

The results (Fig. 6) clearly show that the NH_4^+ binding model can successfully explain the commonality among the three classes of ALS inhibitors. The NH_4^+ ion is located at the same position relative to the azine moiety and can interact with each inhibitor. The three types of acidic moiety can bind to the NH_4^+ ion in different ways. In the case of **3**, negative charge is mainly located at the oxygens of the COO^-. In the anionic

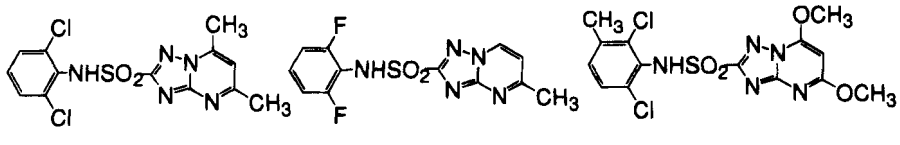

Fig. 3. Chemical structures of triazolopyrimidine herbicides.

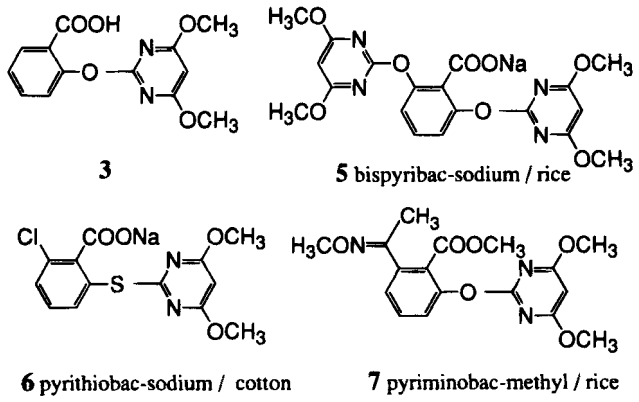

Fig. 4. Chemical structures of pyrimidyl ether herbicides.

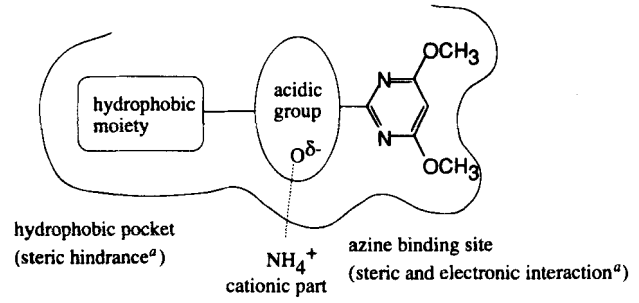

Fig. 5. Hypothesized receptor mapping of ALS inhibitors. [a] Investigated in ref. 5.

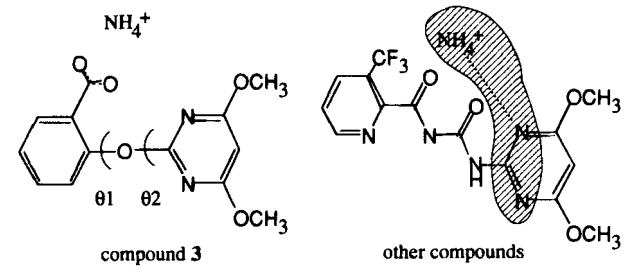

Fig. 6. Geometry optimization of NH_4^+ binding model. The angles $\theta 1$ and $\theta 2$ of compound **3** were kept unchanged. The shaded parts were unchanged in other compounds.

form of **2** that results from deprotonation of the NH group, the negative charge is not on the nitrogen but mainly on the oxygens of the SO_2 group, which can interact with the NH_4^+ ion. In the case of **1**, the negative charge of the SO_2N^- CO group is delocalised on the three oxygens and these atoms can chelate with the NH_4^+ ion. Although the three-dimensional location of these anionic moieties is different, it is possible that the anionic groups bind to the same cationic moiety of ALS.

3 JUSTIFICATION OF MODEL

3.1 Structure–activity relationship data

SAR information was retrieved from the structural database in our laboratory or obtained from the literature. In-vivo herbicidal testing in our laboratory involves a number of plant species including soybean, cocklebur, morning glory, smart weed, pig weed, corn, rice, wheat and barnyard grass. Compounds are sprayed directly onto the leaves and assessments are made after one or two weeks. The data were used to classify compounds as highly active, weakly active or inactive. These classes correspond approximately to activity at less than 125 g ha^{-1}, activity between 125 g ha^{-1} and 500 g ha^{-1}, and activity only at greater than 500 g ha^{-1}.

3.2 Energy parameters

The action of an inhibitor can be broken down into three components. The first of these is the dissociation of the neutral inhibitor. Most of the compounds under consideration are known to exist in their anionic forms in solution at physiological pH, whereas gas-phase calculations of the deprotonation would, of course, give large unfavourable enthalpy changes. Attention was therefore focused on the other two processes. The first of these is the conformational change that the (anionic) inhibitor must undergo in order to achieve its binding conformation. The final process is the favourable binding interaction the inhibitor makes with the NH_4^+ ion.

The AM1 method was employed for all energy calculations. An NH_4^+ binding model of each compound was obtained in a similar manner to **1** and **3**. Geometries of the active conformations of the anions were obtained by removing the NH_4^+ from the NH_4^+ binding models and optimising internal coordinates other than the torsional rotation of single bonds. Stable conformations of the anions were obtained, optimising all internal coordinates fully.

Thus, for each inhibitor, the following energy parameters were obtained.

$$\Delta H_{bind} = \Delta H(NH_4^+ \text{ anion complex}) - \Delta H(\text{active anion}) - \Delta H(NH_4^+) \quad (3.1)$$

$$\Delta H_{conformation} = \Delta H(\text{active anion}) - \Delta H(\text{stable anion}) \quad (3.2)$$

These energy parameters ignore important aspects of the molecular process in the liquid phase. In particular, ion–dipole intramolecular interactions are likely to be overestimated in such calculations. However, as discussed below, these energy parameters should reflect crucial features of the inhibitor action at a molecular level.

3.3 Substituent effects of the hydrophobic moiety

In a QSAR study of pyridinesulfonylureas, it was reported than the 6-position of the pyridine ring is most

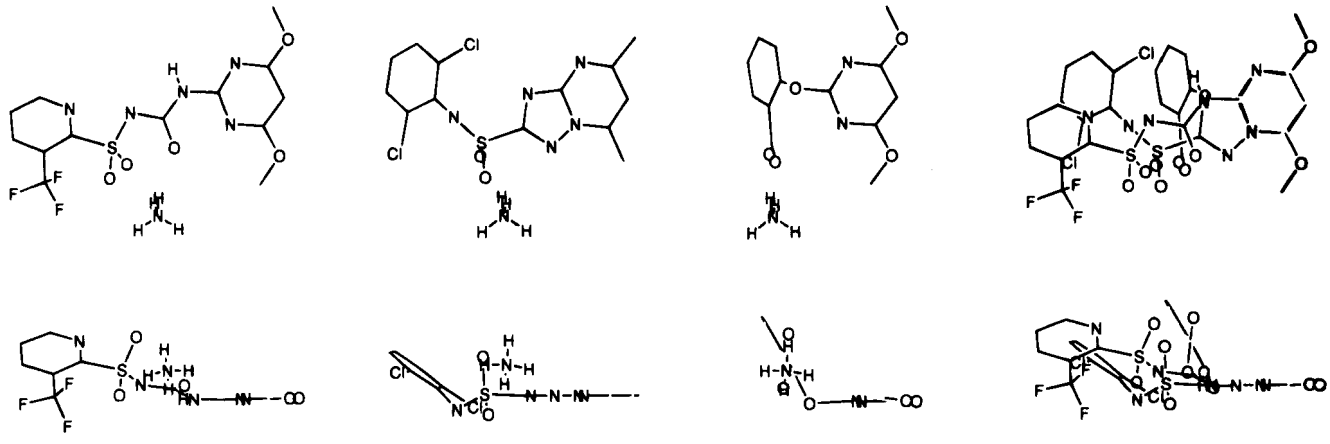

1 2 3 superimposition

Fig. 7. Three-dimensional structures of NH_4^+ binding models. The upper and lower rows are projections to x–y and y–z planes, respectively.

amenable to substitution.[6] Figure 7 helps to explain this SAR. The space around the 6-position of **1** was occupied by **2**, while the space near the 4- or 5-position was occupied only in **1**. This suggests the existence of a pocket near the 6-position of pyridinesulphonylureas. Figure 7 shows that the space near the 3-position of **2** is also occupied by **1**, and hence should be sterically accessible. Structure **4** (Fig. 3) is a 3-substituted analogue of **2** that was a development compound. The space around the 3-position of **3** is occupied by **1** and **2**. Therefore it was reasonable that this position was substituted in other development compounds (**5**, **6** and **7**, Fig. 4).

TABLE 1
Structure–Activity Relationships of Sulfonylurea and Related Compounds

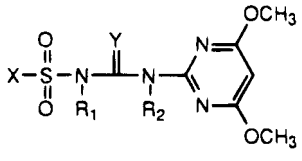

X	*Y*	R_1	R_2	*Activity*[a]
Aryl	O	H	H	O
Aryloxy	O	H	H	O
Substituted amino	O	H	H	O
Aryl	NR_3	H	H	Δ
Aryl	S	H	H	Δ
Aryl	O	H	CH_3	O-Δ
Aryl	O	CH_3	H	X
Aryl	O	CH_3	CH_3	X
Aryl	SO_2NHCH_2CONH			X
Aryl	$SO_2NHNHCONH$			X
Aryl	$SO_2NHCONHNH$			X
Aryl	SO_2CH_2CONH			X
Aryl	$SO_2NHC(CH_3)_2OCONH$			X
Aryl	$NHCONHSO_2$			X
Aryl	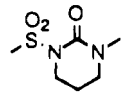			X

[a] Herbicidal activity. O, highly active; Δ, weakly active; X, inactive.

3.4 Structure–activity relationships of sulfonylureas and related compounds

SAR information for a series of molecules all containing the sulfonylurea bridge are listed in Table 1 (results from our laboratory). When X is a suitably substituted aromatic ring, aryloxy group or amino group, strong or weak herbicidal activity is observed. R_2 can be methylated without diminishing activity, but methylation at R_1 results in inactive compounds. For Y, oxygen is the preferred atom, nitrogen or sulfur being less active. Replacement of the SO_2NHCO by SO_2NHCH_2CO, $SO_2NHNHCO$, SO_2CH_2CO or $SO_2NHC(CH_3)_2OCO$, results in inactive compounds. Compounds with an $SO_2NHCONHNH$ or $NHCONHSO_2$ bridge instead of the $SO_2NHCONH$ bridge of SUs are inactive. The location of the SO_2NHCO group with respect to the azine is significantly different in these compounds. This structure–activity information suggests that the SO_2NHCO group is located at a suitable position relative to the azine ring and is the essential moiety of the bridge. The SO_2N^-CO group was involved in the binding to NH_4^+ in Fig. 7, which is consistent with the above SAR.

Some model calculations for a sulfonylurea and related compounds are listed in Table 2. The inactivity of **8** with a $CHCCl_3$ group instead of the CO of a sulfonylurea can be explained by the low affinity of its anionic form to NH_4^+ while the low affinity to NH_4^+ and the high conformational activation energy may be responsible for the inactivity of **10**, which has a CO

TABLE 2
Energy Parameters of Sulfonylurea and Related Compounds

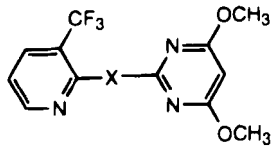

Compound	*X*	*Activity*[a]	$\Delta H_{conformation}$ (*kcal mol*$^{-1}$)	ΔH_{bind} (*kcal mol*$^{-1}$)
1	$SO_2NHCONH$	O	10	108
8	$SO_2NHCH(CCl_3)NH$	X	3	73
9	$SO_2NHCOCH_2$	Δ	2	115
10	CONHCONH	X	8	96
11	$PO(OCH_3)NHCONH$	X	7	109

[a] Herbicidal activity. O, highly active; Δ, weakly active; X, inactive.

group instead of the SO_2 group. It is interesting that compound **9**, which fits the NH_4^+ model equally as well as **1**, shows some herbicidal activity. Thus, although the NH_4^+ binding model was proposed without a detailed knowledge of the SAR at the sulfonylurea bridge, the model is able to explain the SAR successfully. However, since the level of activity of **9** was lower than that of **1**, despite its superior energy parameter values, the NH_4^+ binding model is not quantitative. Compound **11**, which also has favourable energy parameter values, was inactive *in vivo*. However, it showed slight inhibitory activity against ALS enzyme *in vitro* at 10^{-5} M (Akagi, T., unpublished).

3.5 Structure–activity relationships of triazolopyrimidines

Results for two types of triazolopyrimidines are listed in Table 3. Percival[17] reported that optimisation of the structure of **12** led to the structure **2**. This is an interesting result as **12** is more similar to the SUs in chemical structure. The superiority of **2** over **12** can be explained by $\Delta H_{conformation}$ in this study. Compound **2** may be more active because it requires less conformational activation energy in its anionic form. In the atom-by-atom fitting study, the position of the oxygens and the acidic hydrogen of **12** were closer to those of **1** than those of **2**. Thus, the behaviour described in this section can be explained only by the NH_4^+ model.

3.6 Structure–activity relationships of pyrimidyl ethers and related compounds

Results for pyrimidyl ethers and related compounds are listed in Table 4. It is notable that **13** is inactive, even though **13** is an amino bridge analogue of **3**. The large $\Delta H_{conformation}$ of **13** suggests a reason for its inactivity.

TABLE 3
Energy Parameters of Triazolopyrimidines

Compound		$\Delta H_{conformation}$ (*kcal mol*$^{-1}$)	ΔH_{bind} (*kcal mol*$^{-1}$)
12	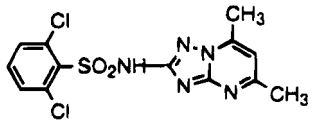	4	98
2	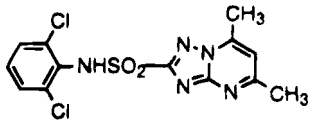	1	98

TABLE 4
Energy Parameters of Pyrimidyl Ethers and Related Compounds

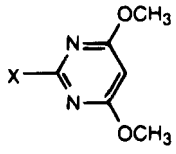

Compound	*X*	*Activity*[a]	$\Delta H_{conformation}$ (*kcal mol*$^{-1}$)	ΔH_{bind} (*kcal mol*$^{-1}$)
3	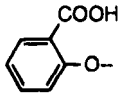	O	8	109
13	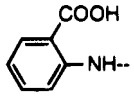	X	16	—
14	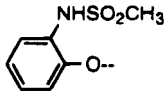	Δ	7	110
15	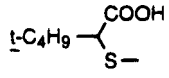	O	2	110
16	t-C_4H_9CONH—	X	0	87
17	$C_2H_5OCONHO$—	X	1	89
18	$HOCOCH_2CH_2S$—	Δ	7	122
19	$HOCOC(CH_3)_2S$—	X	4	109

[a] Herbicidal activity. O, highly active; Δ, weakly active; X, inactive.

The planarity of the conjugated amino group as well as the intramolecular hydrogen bond between the amino group and the carboxylic group makes this compound rather rigid and therefore it is difficult for it to adopt the active conformation. In compound **14**, the SO_2NH group can deprotonate to SO_2N^-, which can bind to the NH_4^+ in a similar manner to the COO^- group of **3**, thus supporting the idea that the SO_2NH and COOH groups can function similarly when placed in an appropriate position. The herbicidal activity of **15** is also high, which is consistent with the favourable energy parameters. This compound, as well as the third entry of Table 1, suggests that aliphatic groups can be alternatives to the aromatic ring in the hydrophobic moiety. The inactivity of **16** and **17** (Table 4) can be explained by their low ΔH_{bind}. On the other hand, the inactivity of compound **18** is not explained by the NH_4^+ binding model. This compound is the only serious exception in this study. Some unknown factors such as steric hindrance or transport may interfere with the binding of this compound.

3.7 Structure–activity relationships of other ALS inhibitors

Results for other compounds with an acidic group and an azine moiety are listed in Tables 5 and 6. Results in Table 5 are from our laboratory. Compound **20** exhibited slight herbicidal activity, while other compounds were inactive. Here again, compounds **21**, **22** and **23** with low affinity to the NH_4^+ are inactive. Compounds in Table 6 are taken from the literature.[17–19] Compound **25** shows herbicidal activity. Moreover, it is reported that some analogues exhibit very strong herbicidal activity at rates down to 5–10 g ha^{-1}.[17] Such high activities are consistent with the energy parameters in the binding model.

Compounds **26**[18] and **27**[19] are ALS inhibitors with high potency. The reported I_{50} values of these compounds are 10^{-8} and 10^{-7} M, respectively. Energy parameters of these potent compounds were also favourable. As the structures of these compounds were published after most of the calculations in this study

TABLE 5
Energy Parameters of Other Compounds (1)

Compound		*Activity*[a]	$\Delta H_{conformation}$ (*kcal mol*$^{-1}$)	ΔH_{bind} (*kcal mol*$^{-1}$)
20	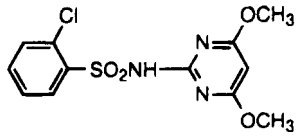	Δ	0	95
21	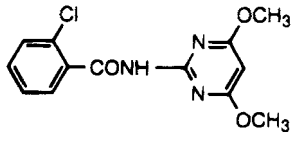	X	0	65
22	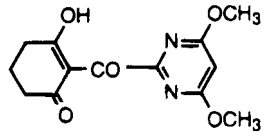	X	1	50
23	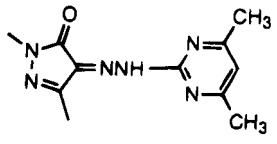	X	0	88

[a] Herbicidal activity. O, highly active; Δ, weakly active; X, inactive.

TABLE 6
Energy Parameters of Other Compounds (2)

Compound		$\Delta H_{conformation}$ (*kcal mol*$^{-1}$)	ΔH_{bind} (*kcal mol*$^{-1}$)
24	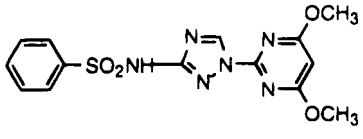	1	111
25	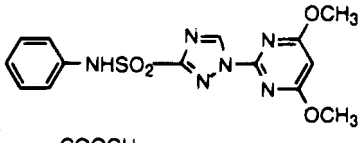	0	106
26	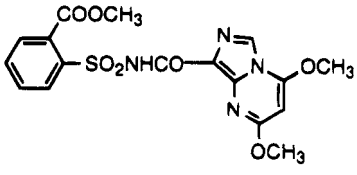	3	106
27	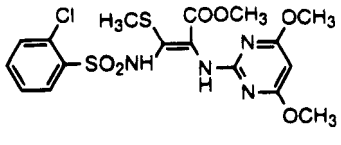	9	106

were finished, they serve as additional proof of the applicability of the NH_4^+ binding model.

4 USE OF MODEL FOR PHARMACOPHORE SEARCH

The usefulness of the NH_4^+ binding model for searching for novel ALS inhibitors was investigated as a way of confirming the reliability of the model. Attention was focused on functional groups with double-bonded oxygens, such as carbonyl, sulfonyl and nitro as likely 'binding atoms' that could interact with the NH_4^+. About 60000 monovalent substructures with a double-bonded oxygen were generated from around 3000 molecular structures available to us. Chemical structures of these compounds were taken from several reviews and reports. Each monovalent substructure was connected at the 2-position of the 4,6-dimethoxypyrimidine ring and the connecting bond was rotated from 0° to 360° by increments of 15°. Geometrical conditions (Fig. 8) were applied to screen structures that were able to fit the NH_4^+ binding model. These conditions were:

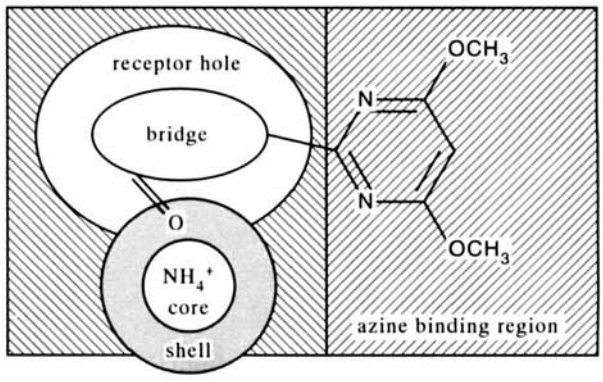

Fig. 8. Geometrical conditions for substructure searching which fit the NH_4^+ binding model.

(1) The double-bonded oxygen was located in the region of the NH_4^+ where the distance from the nitrogen of the NH_4^+ was between 2·6 A and 2·9 A.

(2) No heavy atoms were located close to the NH_4^+,

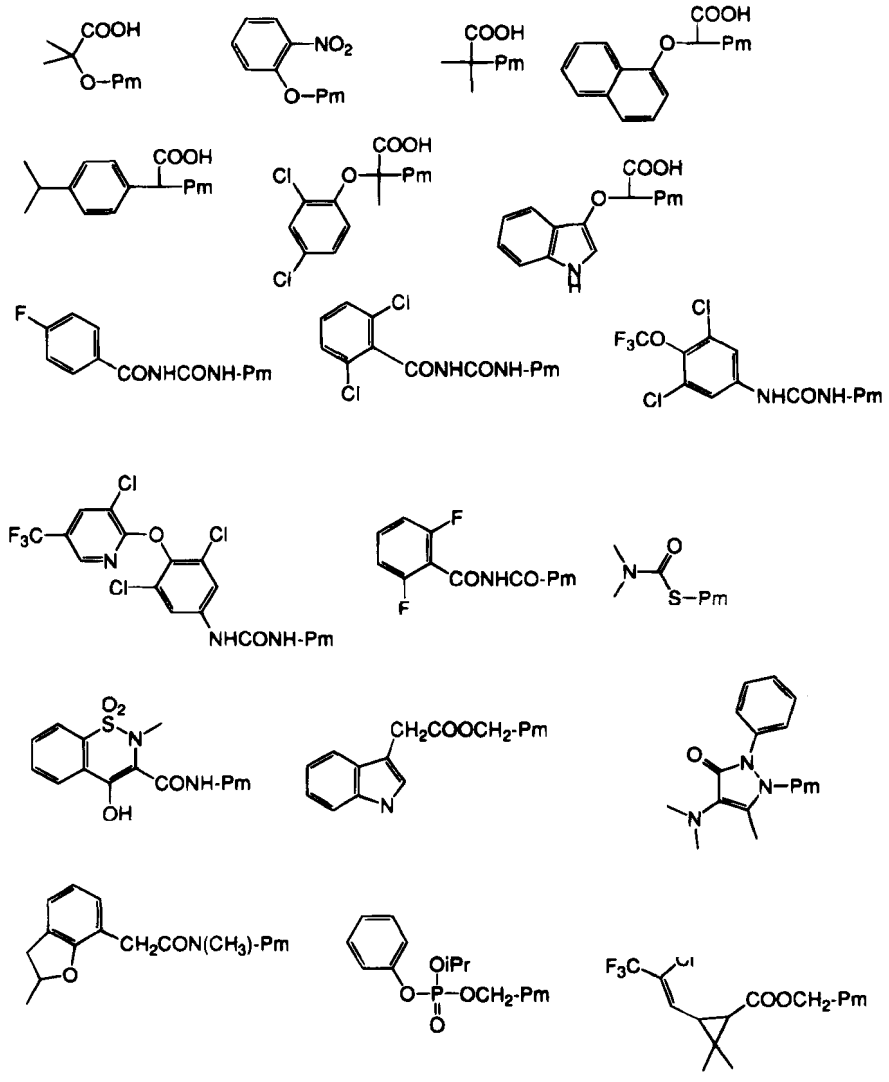

Fig. 9. Output of drug design procedure. Pm in the figures means 4,6-dimethoxypyrimidine.

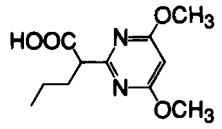

Fig. 10. Chemical structure of **28**.

such that the distance from the nitrogen was less than 1·17 A plus the van der Waals radius of the heavy atom.

(3) No heavy atoms were located on the pyrimidine side of the connecting bond.

(4) All atoms on the path between the double-bonded oxygen and the pyrimidine ring had to be located within a distance of 1 A from any atom of the NH_4^+ binding model of **1**, **2** or **3**.

(5) The substituents had to consist of between 12 and 35 atoms.

The first and second conditions are essential for the favourable interaction between the candidate structure and the NH_4^+. The third condition is necessary to avoid interference to the binding at the azine moiety. The fourth condition was added to minimise the difference in shape from **1**, **2** or **3**. The last condition is not a requirement, but was added for convenience of calculation. Conditions about the acidic proton, which would dissociate leaving the oxygen negatively charged, were not included.

About 1000 substructures (including some duplicates) were selected by applying these conditions. Some of the results are shown in Fig. 9. Since energy calculations are not involved in the selection process, the results are rather noisy. For example, compounds with benzoylurea bridges, whose inferiority was discussed in Section 3.4, are included in Fig. 9. As with all pharmacophore searches, the output is intended only as a first attempt to select interesting structures, which can then be considered in more detail. Many compounds with a pyrimidyl ether moiety were generated from this study, two of them being included in the figure. It is interesting that a phenyl pyrimidyl with a nitro group at the 2-position of the benzene ring was proposed. When the nitro group of this compound was replaced by COO^-, which is a bioisoster of the nitro group, compound **3** is obtained.

Additionally, compounds with a carboxylic acid group at the α-position to pyrimidine were selected many times. This skeleton appeared to be novel at that time. However, compound **28** (Fig. 10)[20] with this skeleton has since been published.

5 INTERPRETATION OF MODEL

In this study, the NH_4^+ binding model was derived assuming SUs, TPs and PEs bind in the same receptor site of ALS. IMs were discarded from consideration since they showed little if any substructural similarity. Recently, it has been reported that the inhibiting behaviours of SUs, TPs and PEs are similar (partially competitive to the substrate) while that of IMs is different (non-competitive to the substrate).[21] Moreover, a study of cross-resistance among ALS inhibitors revealed that the resistant biotypes of *Stellaria media* (L.) Vill, against an SU are also highly resistant to a TP but rather susceptible to an IM.[22] Thus our working hypothesis to omit the IMs appears justified.

A low-level MO calculation (semi-empirical AM1) in gas phase was employed for the energy parameters. Moreover, in-vivo rather than in-vitro activities were used to obtain the SAR. It is impressive to note that such a simple model can explain many aspects of the SAR of ALS inhibitors. Thus it seems likely our simple model reflects the important molecular aspects of ALS–inhibitor interactions.

No crystallographic data exist on inhibitor–receptor binding of ALS inhibitors. However, some speculation can be made. Schloss *et al.*[23] reported that ubiquinone-0 or -1 inhibited the isozyme of ALS in *Escherichia coli* in a competitive manner with an SU compound. The binding of ubiquinone-0 or -1 was examined since pyruvate oxidase (POX), which is homologically similar to ALS, requires a quinone as a cofactor, although ALS does not need quinones in its catalytic actions. Thus these authors hypothesised that ALS left some cavity for SUs in its evolution from POX. It is interesting that the *s*-triazine type herbicides that inhibit the Hill reaction also bind to the same cavity as plastoquinone, in the photoreaction centre.[24] From the substructural similarities between the *s*-triazine herbicides and the SUs and among the quinones, it can be suggested that the azine moiety of SUs, TPs and PEs binds to the 'quinone-binding site' of ALS enzyme by some interaction similar to that of the *s*-triazine herbicide in the photoreaction centre. On the other hand, since the substrate of ALS (pyruvate) is anionic, it seems reasonable to assume that the enzyme contains a positive charge that attracts the substrate in the catalytic centre; this cationic centre is represented by the NH_4^+ ion in this study.

ACKNOWLEDGEMENT

The author wishes to thank Dr Christopher J. Palmer for critical reading.

REFERENCES

1. Stetter, J. (ed.) Herbicides Inhibiting Branched Chain Amino Acid Biosynthesis *Chemistry of Plant Protection* 10, Springer, 1994.

2. Levitt, G., Sulfonylureas: New high potency herbicides. In *Pesticide Chemistry: Human Welfare and Environment* 1, ed. J. Miyamoto & P. C. Kearney. Pergamon Press, Oxford, 1982, pp. 243–50.
3. Hay, J. V., Chemistry of sulfonylurea herbicides. *Pestic. Sci.*, **29** (1990) 247–62.
4. Brown, H. M., Mode of action, crop selectivity and soil relations of the sulfonylurea herbicides. *Pestic. Sci.*, **29** (1990) 263–82.
5. Murai, S., Nakamura, Y., Akagi, T., Sakashita, N. & Haga, T., Synthesis and quantitative structure–activity relationships of pyridylsulfonylurea herbicides. In *Synthesis and Chemistry of Agrochemicals No. 3 ACS Symposium series* 504. ed. D. R. Baker, J. G. Fenyes & J. J. Stefens. Am. Chem. Soc. Washington, 1992, pp. 41–55.
6. Ishida, Y., Ohta, K., Itoh, S., Nakahama, T. Miki, H. & Yoshikawa, H., Synthesis of novel herbicidal sulfonylurea compounds with imidazo[1,2-*a*]pyridine moiety. *Nihon Noyaku Gakkaishi* (*J. Pestic. Sci.*), **18** (1993) 175–82.
7. Wepplo, P., Imidazolinone herbicides: Synthesis and novel chemistry. *Pestic. Sci.*, **29** (1990) 293–318.
8. Ladner, D. W., Structure–activity relationships among the imidazolinone herbicides. *Pestic. Sci.*, **29** (1990) 317–34.
9. Kleschick, W. A., Costales, M. J., Dunbar, J. E., Meikle, R. W., Monte, W. T., Pearson, N. R., Snider, S. W. & Vinogradoff, A. P., New herbicidal derivatives of 1,2,4-triazolo[1,5-*a*]pyrimidine. *Pestic. Sci.*, **29** (1990) 341–56.
10. Shimizu, T., Nakayama, I., Nakao, T., Nezu, Y. & Abe, H., Inhibition of plant acetolactate synthase by herbicides, pyrimidylsalicylic acids. *Nihon Noyaku Gakkaishi* (*J. Pestic. Sci.*), **19** (1994) 59–67.
11. Takahashi, Y., Akagi, T. & Sasaki, S., Three-dimensional pharmacophoric pattern search using COMPASS: Nootropic agents. *Tetrahedron Computer Methodology*, **3** (1990) 27–35.
12. Akagi, T. & Sakashita, N., A quantum chemical study of light-dependent herbicides. *Z. Naturforsch.*, **48c** (1993) 345–9.
13. Dewar, M. J. S., Zoebish, E. G., Hearly, E. F. & Stewart, J. J., AM1: A new general purpose quantum mechanical model. *J. Am. Chem. Soc.*, **107** (1985) 3902–9.
14. Barino, L., Use of a least-squares best molecular fit routine in a steric comparison of flexible molecules. *Computer & Chemistry*, **5** (1981) 85–90.
15. Lasbanowski, J., Motoc, I., Naylor, C. B., Mayer, D. V. & Dammkoehler, R. A., Three-dimensional quantitative structure–activity relationships. 2. Conformational mimicry and topological similarity of flexible molecules. *Quant. Struct.-Act. Relat.*, **5** (1986) 138–52.
16. Clark, M., Cramer III, R. D. & Opdenbosch, N. V., Validation of the general purpose tripos 5.2 force field. *J. Comput. Chem.*, **10** (1989) 982–1012.
17. Percival, A., New heteocyclic herbicidal sulphonamides. *Pestic. Sci.*, **31** (1991) 569–80.
18. McFadden, H. G. & Huppatz, J. L., Vinylogues sulfonylureas: A new class of acetohydroxyacid synthase inhibitors incorporating a large bridging moiety. *Z. Naturforsch.*, **48c** (1993) 356–63.
19. Tseng, C. P., Frinkelstein, B. L., Kerschen, J. A. & Schneiders, G. E., Synthesis and herbicidal activity of pyrazolo[1,5-*a*]pyrimidine-3-carboxylic sulfonamides and related heterocyclic carbonylsulfonamides. In *7th ICPC Congress Hamburg* (1990) 01A–75.
20. Harde, C., Heinrich, J. G., Jones, G. P., Kotter, C., Kruger, A., Kruger, G., Nordhoff, E., Rees, R., Tarara, G. & Wegner, P., Substituted 2-pyrimidinyl-acetic acid derivatives, and their use as herbicides, fungicides and plant growth regulators. *US Pat.* US-5238907, 1992.
21. Shimizu, T., Nakayama, I., Wada, N. & Abe, H., Kinetic studies on the inhibition of acetolactate synthase pyrimidylsalicylic acids. *Nihon Noyaku Gakkaishi* (*J. Pestic. Sci.*), **19** (1994) 257–66.
22. Devine, M. D., Marles, M. A. S. & Hall, L. M., Inhibition of acetolactate synthase in susceptible and resistant biotypes of *Stellaria media*. *Pestic. Sci.*, **31** (1991) 273–80.
23. Schloss, J. V., Ciskanik, L. M. & Van Dyk, D. E., Origin of the herbicide binding site of acetolactate synthase. *Nature* (*London*), **331** (1988) 360–2.
24. Michel, H., Epp, O. & Deisenhofer, J., Pigment-protein interaction in the photosynthetic reaction centre from *Rhodopseudomonas viridis*. *EMBO J.*, (1986) 2445–51.